Acta Cryst. (1987). B43, 548-554

Restrained Least-Squares Refinement of the Crystal Structure of the Ribonuclease T_1 * 2'-Guanylic Acid Complex at 1·9 Å Resolution

BY RAGHUVIR ARNI, UDO HEINEMANN, MARIA MASLOWSKA, RYOJI TOKUOKA AND WOLFRAM SAENGER

Institut für Kristallographie, Freie Universität Berlin, Takustrasse 6, D-1000 Berlin 33, Federal Republic of Germany

(*Received* 21 *April* 1987; *accepted* 7 *July* 1987)

Abstract

The crystal structure of the enzyme ribonuclease T_1 complexed with the specific inhibitor 2'-guanylic acid has been refined to an R value of 0·180 by the restrained least-squares method using synchrotron film data in the 6·0–1·9 Å resolution range. The refinement was based on a complete model of the protein derived from a multiple-isomorphous-replacement electron density map at 2·5 Å resolution. Improvement of the protein model involved 15 model-building sessions with *FRODO* on a vector graphics system and 138 cycles of stereochemically restrained refinement. The refined model consists of 777 protein atoms, 24 inhibitor atoms, and 91 water O atoms. All protein atoms could be located except for the side chain of residue Glu102. The mean temperature factor for protein atoms is 12·3 $Å^2$ and the r.m.s. deviation of bond lengths from ideal values is 0·018 Å. The r.m.s. distance of main-chain atoms from their equivalents in the unrefined model is 1·38 Å. Intermolecular lattice contacts in space group $P2_12_12_1$ comprise eight possible hydrogen bonds between protein atoms, mostly involving the polypeptide backbone of the protein, and 62 non-bonded contacts of atoms within 4·0 Å of each other. In addition, there are 13 water molecules connecting symmetry-related protein molecules *via* hydrogen bonds. The bound inhibitor does not participate in intermolecular contacts but several protein active-site groups are involved in lattice contacts.

Introduction

Ribonuclease (RNase) T_1 from the fungus *Aspergillus oryzae* is a small and stable enzyme of 104 amino-acid residues and molecular mass 11 085 daltons that hydrolyzes single-stranded ribonucleic acid by specifically cleaving the phosphodiester bonds on the 3' side of guanosine nucleosides. As in the case of bovine pancreatic ribonuclease, the reaction proceeds *via* a 2',3'-cyclic phosphodiester intermediate to yield oligonucleotides with terminal nucleoside 3'-monophosphates. 2'-Guanylic acid (2'GMP) is the most potent competitive inhibitor of RNase T_1, characterized by binding to the protein at pH 5 in a 1:1 ratio with a dissociation constant of 6·5 μM (Egami, Oshima & Uchida, 1980; Takahashi & Moore, 1982).

Genes coding for RNase T_1 have been chemically synthesized and expressed by two groups (Ikehara, Ohtsuka, Tokunaga, Nishikawa, Uesugi, Tanaka, Aoyama, Kikyodani, Fujimoto, Yanase, Fuchimura & Morioka, 1986; Quaas, Choe, Hahn, McKeown, Stanssens, Zabeau, Frank & Blöcker, 1987). The crystal structure of the protein refined at high resolution will help these groups to define target sites for mutations aimed at clarifying specific points of dispute regarding the function of the enzyme.

A model for the complete three-dimensional structure of RNase T_1 complexed with 2'GMP has been derived from a 2·5 Å multiple-isomorphous-replacement (MIR) electron density map (Heinemann & Saenger, 1982). Sugio, Amisaki, Ohishi, Tomita, Heinemann & Saenger (1985) have given a short account of the structure of the RNase T_1 * 2'GMP complex crystallized at a lower pH and refined at 1·9 Å resolution. The structure of 3'GMP when bound to RNase T_1 has also been determined (Sugio, Oka, Ohishi, Tomita & Saenger, 1985).

Here we describe the refinement at 1·9 Å resolution by the stereochemically restrained least-squares method of the RNase T_1 * 2'GMP complex and present an analysis of the crystal packing. A full description of the molecular structure and a discussion of its biochemical implications will be given elsewhere (Arni, Heinemann, Tokuoka & Saenger, 1987).

Experimental

The protein used in this study was the isoenzyme of RNase T_1 (Heinemann & Saenger, 1982), where a lysine residue replaces Gln25 of native RNase T_1 (Takahashi, 1985; Kratzin, 1987). The protein was isolated by the method of Fülling & Rüterjans (1978) and crystals were grown as described (Heinemann, Wernitz, Pähler, Saenger, Menke & Rüterjans, 1980) but employing vapor diffusion rather than microdialysis techniques.

0108-7681/87/060548-07$01.50

Table 1. *Statistics of intensity data*

$R_{merge} = \sum|I - \langle I\rangle|/\sum I$. Values in parentheses are standard deviations.

Space group		$P2_12_12_1$ (No. 19)
Lattice constants (Å)	a	46·81 (3)
	b	50·11 (3)
	c	40·44 (2)
Total number of reflections measured		23 819
Reflections with negative intensities		117
R_{merge}		0·088
Unique reflections	$F_o \geq 1\sigma(F_o)$	6788
	$F_o \geq 2\sigma(F_o)$	6687
	$F_o \geq 3\sigma(F_o)$	6349

Data acquisition

In the early stages of refinement, the data collected on a diffractometer to 2·5 Å resolution (Heinemann & Saenger, 1982) were used. For high-resolution refinement a 1·9 Å data set was collected from a single crystal (~2×0·2×0·2 mm) using an Arndt–Wonacott camera at the synchrotron source DESY (Hamburg). During the measurement at the X31 station (HASYLAB) of the European Molecular Biology Laboratory, the X-ray beam was tuned to a wavelength of 1·488 Å.

The crystal was mounted with its long dimension (c axis) along the capillary and rotated with angular increments of 3° covering a total range of 90°. The crystal-to-film distance was set to 55 mm. Using a 0·5 mm collimator, only part of the needle-shaped crystal was irradiated at any given time. In order to minimize radiation damage, the crystal was moved laterally between exposures, irradiating for equal time all volume elements of the crystal. Diffraction data in the blind region of reciprocal space were not measured, since re-mounting of the crystal in the capillary for oscillation about a different axis was not feasible. Data were recorded on Kodak DEF 2 film using three films per cassette.

The diffraction data from oscillation films were digitized on an off-line Optronics P-1000 rotating-drum scanner operated with a 100 μm grid in the 2 OD range. For data processing, the Cambridge suite of programs (Machin, Wonacott & Moss, 1983) was used. Cell constants, crystal orientation and camera constants were refined against 130 reflections on six still photographs. An overall temperature factor (Wilson, 1942) of 14·9 Å^2 was obtained for the 6788 unique observed reflections of the data set which represents 93% of the reflections expected at 1·9 Å resolution. Data acquisition and processing statistics are summarized in Table 1.

Structure refinement

The starting model

Structure refinement started from a Kendrew wire model that had been fitted into a 2·5 Å resolution electron density map by means of an optical comparator [Richards box in the version of Colman, Jansonius & Matthews (1972)]. The map had been phased by multiple isomorphous replacement making use of both isomorphous and anomalous differences provided by two independent derivatives [Pb^{2+} and $Pt(NH_3)_4^{2+}$] and their cross derivative. Phasing statistics yielded a mean figure of merit $\langle m\rangle = 0{\cdot}749$ (Heinemann, 1982; Heinemann & Saenger, 1982). The MIR map was of good quality and could be used as a reference throughout the refinement.

The model for the RNase T_1 * 2′GMP complex as obtained from the MIR map contained all atoms except for the side chain of Lys41 where no density was present. The inhibitor molecule was clearly defined and distinct from the protein. An error in the published sequence of RNase T_1 (Takahashi, 1971) which was corrected later (Pro71-Gly72-Ser73 to Gly71-Ser72-Pro73; Takahashi, 1985) was not detected at this stage. Coordinates were obtained from the model with the plumb-line method. The inaccuracies of the starting model owing to misinterpretations of the electron density at selected regions and the crude method of coordinate extraction were reflected in a considerably scattered distribution of φ, ψ values in the Ramachandran plot.

Course of the refinement

The structure of the RNase T_1 * 2′GMP complex was refined by the stereochemically restrained least-squares method (Hendrickson & Konnert, 1980; Hendrickson, 1985) in 15 rounds. Each round of refinement involved a session of model building using the program *FRODO* (Jones, 1978; modified by J. Pflugrath) on an Evans and Sutherland PS300 colour graphics system followed by several cycles of least-squares refinement. Various types of Fourier maps were used in the model-building process; standard difference Fourier maps with coefficients $(F_o - F_c)\exp i\alpha_{calc}$ proved more useful towards the end of refinement while double difference Fourier maps using $(2F_o - F_c)\exp i\alpha_{calc}$ were used throughout. In fragment-deleted ('omit') difference Fourier maps, which were used frequently in the early stages of refinement, no more than six amino-acid residues (about 5% of the structure) were left out of the calculation of structure factors in order to retain a readily interpretable map. In addition, $(3F_o - 2F_c)\exp i\alpha_{calc}$ maps and the MIR electron density map were consulted. An ideal model for the bound inhibitor 2′GMP was constructed on the basis of the crystal structure of 5′GMP.7H_2O (Katti, Seshadri & Viswamitra, 1981) using the program *CONNEXN* (A. Pähler & W. A. Hendrickson, unpublished).

The first stage of refinement (rounds 1–4) involved extensive model building and the gradual extension of resolution. During the second stage (rounds 5

and 6), atomic isotropic temperature factors were introduced into the refinement process. The inclusion of solvent atoms began with round 7. At the start of each round of refinement, a few trial cycles were carried out to determine the weighting parameters. The weighting factors for the diffraction terms were set to one half the average discrepancy between observed and calculated amplitudes as suggested by Hendrickson (1985). During the later stages of refinement the structure-factor weights were changed and a minimum threshold value of 25 was used. This rather conservative approach was used since the e.s.d.'s do not take into account systematic errors, for example due to absorption, and it was felt that they were unrealistically low in some cases. In the last rounds of refinement the bond-length and bond-angle weights were tightened to improve the stereochemistry of the model. The progress of the refinement is illustrated in Fig. 1 where each arrow indicates the calculation of difference Fourier maps and subsequent model building.

Refinement was initiated using the 2·5 Å resolution data of Heinemann & Saenger (1982). Prior to the least-squares refinement, extensive model building with *FRODO* was performed, placing strong emphasis on correct stereochemistry and omitting several doubtful sections of the protein molecule. The resulting model containing 736 atoms gave a starting R value for the refinement of 0·386. The initial cycle of refinement consisted of stereochemical idealization only.

During round 2, the overall temperature factor was reduced from 16·1 to 14·0 $Å^2$ and the R value in the 5·0–2·5 Å resolution range converged at 0·323 in 13 subsequent cycles. In the next round, the diffractometer data of Heinemann & Saenger (1982) were replaced with the synchrotron data and the resolution

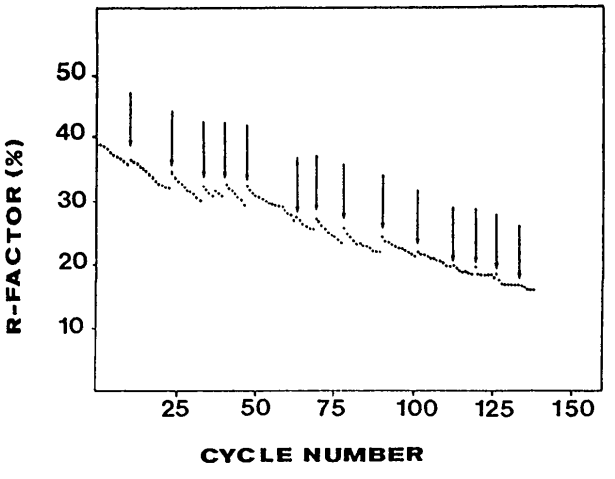

Fig. 1. Variation of the R value ($R = \sum|F_o - F_c|/\sum F_o$, represented by the dots) over the course of the refinement. The refinement was carried out in 15 rounds, each consisting of a model-building session and stereochemically restrained least-squares refinement, as indicated by the vertical arrows.

was extended to 2·2 Å. The R value decreased to 0·300 and the resolution was subsequently extended to 2·0 Å for the next round.

In the second stage of refinement the resolution was extended to the limit of 1·9 Å. Individual temperature factors were introduced but linked together with tight restraints. The R value converged at 0·268.

Improved Fourier maps permitted the unambiguous location of all protein atoms except for the side chain of Glu102 at the beginning of round 7. A difference Fourier map was examined and peaks above a threshold of 0·3 e $Å^{-3}$ were located. Only those peaks that appeared nearly spherical and were not closer than 2·5 Å to protein atoms were accepted as solvent sites and included in the model as neutral water O atoms for further refinement. Initial temperature factors ranging from 15 to 30 $Å^2$ were assigned to the solvent atoms based on their peak heights. The occupancy of solvent atoms was held constant at 1·0. Solvent atoms which refined to B values >50 $Å^2$ were deleted from the model.

At the end of round 10 of the refinement, the solvent structure was scrutinized following the procedure of Fujinaga, Delbaere, Brayer & James (1985). To overcome the bias introduced by the requirement that a potential solvent atom be located in hydrogen-bonding distance to polar protein atoms, all solvent atoms were deleted and redetermined as outlined below. (*a*) All solvent sites were removed from the atom list and protein atoms were subjected to four cycles of restrained refinement. (*b*) A high cut-off level was used for the subsequent Fourier map to relocate solvent atoms. (*c*) The new solvent atoms were allowed to refine for four cycles, and (*d*) a new Fourier map was computed and examined using a lower cut-off. Steps (*c*) and (*d*) were repeated. A high cut-off level proved essential to prevent identification of background noise as solvent. Additional criteria were invoked such as the requirements that the peak height be above a threshold level and that the peak be relatively convex by visual inspection.

After 15 rounds (138 cycles) the refinement converged to an R value of 0·180 for 6349 reflections with $F_o \geq 3\sigma(F_o)$ in the resolution range from 6·0 to 1·9 Å [$R = 0{\cdot}191$ for 6788 reflections with $F_o \geq 1\sigma(F_o)$ in the same resolution range]. The r.m.s. coordinate shift in the last cycle of refinement was 0·015 Å. The highest feature of the final difference electron density map appeared with 0·31 e $Å^{-3}$ and only six peaks exceeded 0·25 e $Å^{-3}$, most of which were close to already assigned solvent peaks, possibly indicating disorder. The mean temperature factor for all atoms of the structure of 14·3 $Å^2$ (12·3 $Å^2$ for protein atoms only) is very close to the overall temperature factor for the data set of 14·9 $Å^2$ determined by Wilson statistics. The weighting parameters and the r.m.s. deviation of the model from ideal values at the end of the refinement are given in Table 2.

Table 2. *Summary of least-squares refinement parameters*

The column 'A.m.s.' lists the deviation of the final model from ideal geometry. Sigma is the inverse square root of the weight applied to the specified type of geometrical restraint. Target sigmas and r.m.s. deviations vary during the course of refinement. All parameters given are those found at the end of the refinement.

Restraints	Sigma	R.m.s.	Number
Distance restraint information (Å)			
Bond distances	0·020	0·018	826
Angle distances	0·030	0·037	1133
Planar 1-4 distances	0·060	0·057	315
Planar groups	0·020	0·015	144
Chiral-centre restraints (Å^3)			
Chiral volumes	0·150	0·150	111
Non-bonded-contact restraints (Å)			
Single torsion contact	0·500	0·191	248
Multiple torsion contact	0·500	0·227	181
Possible H bond	0·500	0·204	71
Conformational torsion angles (°)			
Planar (0, 180)	3·0	2·7	104
Staggered (+/−60, 120)	22·0	21·9	101
Orthonormal (+/−90)	27·0	26·4	17
Isotropic-thermal-factor restraints			
Main-chain bond	1·000	0·917	459
Main-chain angle	1·500	1·494	589
Side-chain bond	1·500	1·880	367
Side-chain angle	2·000	2·744	544
Structure factor			
A term	25·0	28·4	
B term	−50·0	−144·8	

The r.m.s. deviation between the 416 main-chain atoms of the refined model and the coordinates of Heinemann & Saenger (1982) is 1·38 Å, or 1·33 Å after a least-squares superposition of both coordinate sets. The r.m.s. difference is largest in x (0·88 Å) and smallest in y (0·74 Å). Thus, there is no direction with pronounced inaccuracy as is often observed in coordinates obtained from a Richards box. As expected, discrepancies are largest in the loop regions of the protein molecule, especially in the surface region containing the sequence error. Omission of residues 71–73 from the coordinate sets reduces the r.m.s. deviation to 1·25 Å (1·21 Å after least-squares fit). The mean change in the 6·0–2·5 Å resolution range between MIR and final calculated phases of 56·4° is considerably higher than the average phase change of 41·5° that was to be expected from the mean figure of merit $\langle m \rangle = 0{\cdot}749$ for the isomorphous-replacement phasing process (Blow & Crick, 1959).

All computations were carried out on the VAX 11/750 of the Institut für Kristallographie, Freie Universität Berlin. Initially, the program *PROLSQ* (Hendrickson & Konnert, 1980) was used for the restrained least-squares refinement. From round 10 onwards, a modified version became available (*PROFFT*; Finzel, 1987) which accelerates the calculation of structure factors and their derivatives by using fast Fourier transform methods (Agarwal, 1978) in space group $P2_12_12_1$. This program reduced the computing time per cycle from 1 h 31 min 7 s to 8 min 27 s.

Assessment of errors

The assessment of errors in refined crystal structures of macromolecules is not trivial; a discussion of the problems involved has recently been presented by Wlodawer, Borkakoti, Moss & Howlin (1986). The most widely used method to obtain an estimate of the mean coordinate error is that of Luzzati (1952). For the refined crystal structure of the RNase T_1 * 2'GMP complex, the Luzzati plot (Fig. 2) indicates a mean error in atomic coordinates of less than 0·2 Å.

An equally important criterion for the reliability of refined protein structures is the maintenance of proper stereochemistry. This is the reason for the use of stereochemically restrained least-squares refinement, where various geometrical parameters of the molecule being refined are tied with some flexibility to ideal values derived from the crystal structures of amino acids and small peptides. The r.m.s. deviation of the bond lengths of the RNase T_1 * 2'GMP complex from ideality is 0·018 Å, values for other parameters may be taken from Table 2. On a Ramachandran plot (Ramachandran, Ramakrishnan & Sasisekharan, 1963), the torsion angles φ and ψ of all non-glycine residues should fall into the allowed regions, unless forced into alternative conformation by strong intramolecular interactions. As is evident from Fig. 3, only three amino-acid residues of RNase T_1 (Ser37, Asn44 and Asn84) lie outside the region assigned to pleated sheets or α-helix, all of which are involved in hydrogen bonding in tight turns.

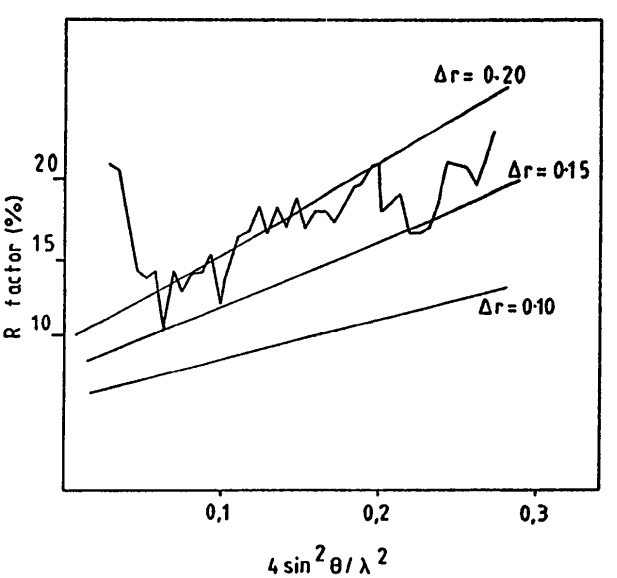

Fig. 2. Estimation of the mean coordinate error by the method of Luzzati (1952). The variation of the crystallographic R factor with resolution is superimposed on theoretical curves calculated for mean coordinate errors Δr of 0·20, 0·15 and 0·10 Å. The observed values fit the theoretical curves reasonably well, indicating a mean coordinate error of less than 0·2 Å.

A tendency of asparagine residues to adopt backbone torsion angles in the left-handed-helix region has been noted earlier (Ravichandran & Subramanian, 1981). It may therefore be concluded that the molecular model of the RNase T_1 * 2'GMP complex possesses reasonable stereochemistry.

Discussion of the refined structure

A complete description of the refined structure is outside the scope of this paper. In the following, we wish to concentrate on features of the protein model that are important for an evaluation of the refinement and to discuss intermolecular contacts between protein molecules in the crystal lattice.

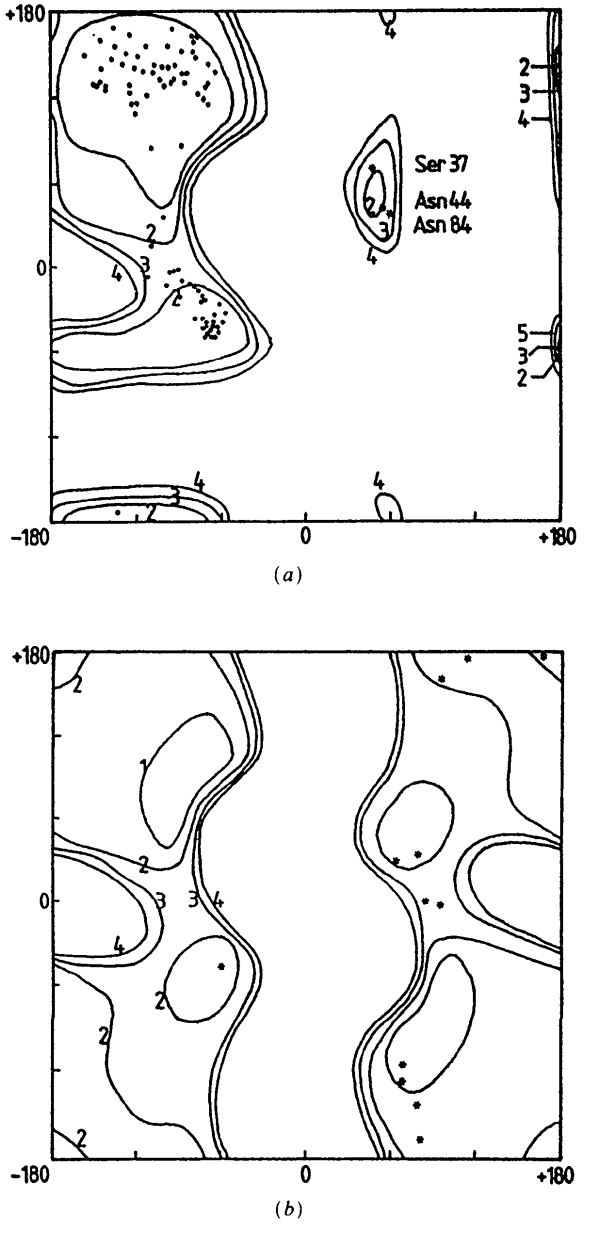

Fig. 3. Backbone-torsion-angle plots for RNase T_1, in the complex with 2'GMP, (*a*) for non-glycine residues, (*b*) for glycine residues only. The conformational energy contours are those of Ponnuswamy & Manavalan (1976).

Molecular structure

Excluding H atoms, the model for the RNase T_1 * 2'GMP complex comprises 777 protein atoms, 24 inhibitor atoms and 91 water molecules.† All protein atoms could be located except for the side chain of residue Glu102 which is not represented by electron density. The bound inhibitor molecule (2'GMP) is clearly seen. All of the solvent sites were assigned as water molecules; occasional attempts during the refinement to identify selected solvent sites as bound cations failed, leading to unreasonable temperature factors. Of the 91 water molecules of the final model, 63 belong to the primary hydration shell of the complex, being within hydrogen-bonding distance (3·5 Å) of polar protein or nucleotide atoms. From the measured crystal density of 1·24 g cm^{-3} (Heinemann, Wernitz, Pähler, Saenger, Menke & Rüterjans, 1980), the total mass per asymmetric unit can be estimated to be 17 700 daltons. Therefore, 4550 daltons, equivalent of 250 water molecules, of bulk-solvent contribution remain unaccounted for.

The only protein atoms missing from the model are C^{γ}, C^{δ}, $O^{\varepsilon 1}$, and $O^{\varepsilon 2}$ of Glu102. Since an error in the sequence (*e.g.* alanine instead of glutamic acid at this position) has been ruled out by resequencing the entire protein (Kratzin, 1987), the side chain of Glu102 must be disordered. It should be mentioned that in the nearly isomorphous complex of RNase T_1 with the dinucleotide guanylyl-(2'→5')-guanosine which is presently being refined in this laboratory, there is electron density for the entire Glu102 residue.

The RNase T_1 molecule consists of a long peripheral α-helix, an extended pleated-sheet structure and several wide loops (Heinemann & Saenger, 1982). The architecture of the protein molecule is reflected in the mobility of the structure characterized by the crystallographic temperature factors (Table 3). Clearly, the loop regions without stabilizing secondary structure are more mobile than the rest of the molecule.

† Atomic coordinates and structure factors have been deposited with the Protein Data Bank, Brookhaven National Laboratory (Reference: 1RNT, R1RNTSF), and are available in machine-readable form from the Protein Data Bank at Brookhaven or one of the affiliated centers at Melbourne or Osaka. The data have also been deposited with the British Library Document Supply Centre as Supplementary Publication No. SUP 37019 (2 microfiche). Free copies may be obtained through The Executive Secretary, International Union of Crystallography, 5 Abbey Square, Chester CH1 2HU, England. At the request of the authors, the list of structure factors will remain privileged until 1 December 1991.

Table 3. *Analysis of temperature factors*

	B (Å^2)	Standard deviation	Number of atoms
Complete structure	14·3	8·1	892
Protein	12·3	4·9	777
Backbone	11·7	4·0	416
Side chains	12·9	5·8	361
Helix	11·7	4·4	124
Sheet	9·7	3·3	301
Other	14·7	5·0	352
2′GMP	18·7	3·4	24
Water	30·4	11·7	91

Table 4. *Intermolecular contacts*

	Possible hydrogen bonds			Non-bonded contacts	
2_1 axis at	from	to	length (Å)	4·0 Å^2	3·5 Å^2
$x=\frac{1}{4}, y=\frac{1}{2}$	Tyr45 O^{η}	Asn83 $N^{\delta 2}$	2·73	6	2
$y=\frac{3}{4}, z=\frac{1}{2}$	Ser35 O^{γ}	Phe100 O	2·51	20	3
$x=\frac{1}{2}, z=\frac{1}{4}$	Gly30 O	Asn9 $N^{\delta 2}$	3·43	6	1
	Gly30 O	Ser63 O^{γ}	2·49		
$x=\frac{3}{4}, y=\frac{1}{2}$	His92 O	Ala1 N	2·65	30	10
	Ala95 O	Ala1 N	2·93		
	Ala95 O	Cys2 N	3·43		
	Gly97 O	Ala1 N	3·06		

Crystal packing

In the orthorhombic unit cell of the RNase T_1 * 2′GMP complex, direct contacts between protein molecules of different asymmetric units are promoted by four 2_1 screw axes, as specified in Table 4. Each protein molecule participates in 62 non-bonded intermolecular contacts between atoms within 4·0 Å of each other, 16 of which involve atom pairs closer than 3·5 Å. In addition, eight contacts shorter than 3·5 Å could be assigned as possible hydrogen bonds. Interestingly, only one hydrogen bond connects protein side chains, while in all other cases the acceptor is a backbone carbonyl O atom and the donors are peptide NH or side-chain groups. The exposed amino terminus of RNase T_1 is the portion of the structure that makes the most intimate contact with neighbouring molecules, the terminal amino group donating three

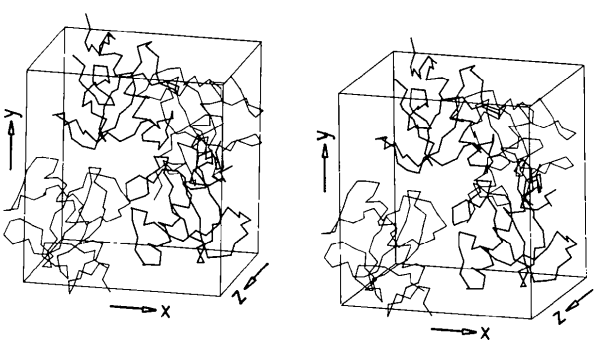

Fig. 4. Packing of RNase T_1 molecules in the unit cell. The four protein molecules that fill the $P2_12_12_1$ cell are represented by C^{α} positions. The two protein molecules at the back of the unit cell have been drawn with heavier lines.

Table 5. *Intermolecular contacts via hydrogen-bonded water*

2_1 axis at $x = 3/4$, $y = 1/2$

Ala1 O		
Asp3 N	Wat106	Gly94 N
Asp3 $O^{\delta 2}$		
Cys10 O		
Asp15 $O^{\delta 2}$	Wat107	Gly94 O
Ser12 O^{γ}		
Ser13 N		
Ser14 N	Wat108	Ser8 O^{γ}
Ser14 O^{γ}		
Cys2 N	Wat180	Gly97 N

2_1 axis at $x = 1/2$, $z = 1/4$

Asp29 O		
Gly30 O	Wat118	Ala75 N
Ser63 N		
Ser63 O^{γ}	Wat119	Gly30 O
Cys6 O		
Ser8 N	Wat178	Glu31 $O^{\varepsilon 1}$

2_1 axis at $y = 3/4$, $z = 1/2$

Asn 36 $N^{\delta 2}$		
Asn 36 $O^{\delta 1}$	Wat120	Glu46 O
Ser 72 O^{δ}		
Gly74 N		
Gly74 O	Wat123	Gly47 O
Gly97 O		
Asn98 $O^{\delta 1}$		
Asn98 $N^{\delta 2}$	Wat124	Asp49 $O^{\delta 1}$
Ser35 N		
Gly71 N		
Gly71 O	Wat129	Glu46 O
Tyr45 O	Wat137	Ser72 N
Ala102 N	Wat193	Ser35 O

intermolecular hydrogen bonds. Fig. 4 gives a stereo representation of the unit-cell contents.

Of the 91 water molecules identified per asymmetric unit, 13 are located within 3·5 Å of polar atoms of two protein molecules and may thus link them *via* hydrogen bonds. Table 5 provides a summary of these bridging water molecules. Several water molecules fully exploit their hydrogen-bonding potential by forming four bonds. In the case of Wat108, which appears to engage in five hydrogen bonds, two donor–acceptor distances are close to the threshold for the assignment of hydrogen bonds (Baker & Hubbard, 1984). Peptide O and N atoms and polar protein side-chain atoms each represent about one third of the hydrogen-bonding partners of water molecules. This underlines the importance of protein-backbone atoms for intermolecular contacts in the crystal of the RNase T_1 * 2′GMP complex.

The bound inhibitor 2′GMP does not participate in lattice contacts. However, the active-site residues Tyr45, Glu46 and His92 are involved in intermolecular contacts, the former predominantly through a hydrogen bond from its O^{η} atom to a symmetry-related Asn83 $N^{\delta 2}$ atom. The potential importance of these interactions has not been fully appreciated in earlier discussions of the active-site geometry of RNase T_1 (Heinemann & Saenger, 1982, 1983).

Since no restraints on intermolecular contacts have been applied during the refinement, the packing analysis also provides an additional check on the

success of the present work. As is evident from Table 4, two rather short hydrogen bonds with donor-acceptor distances of less than 2·6 Å exist. The shortest non-bonded distance is 2·88 Å between C and O atoms; four non-bonded atom pairs closer than 3·2 Å are found.

Concluding remarks

The stereochemically restrained least-squares refinement of the model of the RNase T_1 * 2'GMP complex exemplifies some of the problems in current macromolecular structure refinement. While time spent in diffraction data collection is reduced by using a high-energy synchrotron source and a dramatic saving in computer time is achieved by the incorporation of fast Fourier routines into the Hendrickson-Konnert program (Finzel, 1987), manual model rebuilding on the vector graphics system has become the rate-limiting step in the refinement process. Manual model corrections proved to be absolutely crucial, however, in the course of the RNase T_1 refinement.

The refined model of the RNase T_1 * 2'GMP complex will allow a detailed comparison with the structures of other ribonucleases of the RNase T_1 family (Hill, Dodson, Heinemann, Saenger, Mitsui, Nakamura, Borisov, Tischenko, Polyakov & Pavlovsky, 1983). This model will also be used as the starting point for the refinement of complexes of other substrate analogues with RNase T_1, whose structure analyses are expected to contribute to our understanding of the enzyme's function.

We thank Dr A. Pähler for computer programs and everybody who has helped in diffraction data collection, especially the staff of the outstation of EMBL at DESY in Hamburg. This work was supported by the Deutsche Forschungsgemeinschaft (Sfb 9, Teilprojekt A7).

References

AGARWAL, R. C. (1978). *Acta Cryst.* **A43**, 791-809.

ARNI, R., HEINEMANN, U., TOKUOKA, R. & SAENGER, W. (1987). In preparation.

BAKER, E. N. & HUBBARD, R. E. (1984). *Prog. Biophys. Mol. Biol.* **44**, 97-179.

BLOW, D. M. & CRICK, F. H. C. (1959). *Acta Cryst.* **12**, 794-802.

COLMAN, P. M., JANSONIUS, J. N. & MATTHEWS, B. W. (1972). *J. Mol. Biol.* **70**, 701-724.

EGAMI, F., OSHIMA, T. & UCHIDA, T. (1980). *Mol. Biol. Biochem. Biophys.* **32**, 250-277.

FINZEL, B. C. (1987). *J. Appl. Cryst.* **20**, 53-55.

FUJINAGA, M., DELBAERE, L. T. J., BRAYER, G. D. & JAMES, M. N. G. (1985). *J. Mol. Biol.* **183**, 479-502.

FÜLLING, R. & RÜTERJANS, H. (1978). *FEBS Lett.* **88**, 279-282.

HEINEMANN, U. (1982). *Dreidimensionale Strukturen des Calotropin DI und des Komplexes aus Ribonuclease T_1 und Guanosin-2'-Monophosphat.* PhD Thesis, Univ. of Göttingen, Federal Republic of Germany.

HEINEMANN, U. & SAENGER, W. (1982). *Nature (London)*, **299**, 27-31.

HEINEMANN, U. & SAENGER, W. (1983). *J. Biomol. Struct. Dyn.* **1**, 523-538.

HEINEMANN, U., WERNITZ, M., PÄHLER, A., SAENGER, W., MENKE, G. & RÜTERJANS, H. (1980). *Eur. J. Biochem.* **109**, 109-114.

HENDRICKSON, W. A. (1985). *Methods Enzymol.* **115**, 252-270.

HENDRICKSON, W. A. & KONNERT, J. H. (1980). *Computing in Crystallography*, edited by R. DIAMOND, S. RAMASESHAN & K. VENKATESAN, pp. 13.01-13.23. Bangalore: Indian Academy of Sciences.

HILL, C., DODSON, G., HEINEMANN, U., SAENGER, W., MITSUI, Y., NAKAMURA, K., BORISOV, S., TISCHENKO, G., POLYAKOV, K. & PAVLOVSKY, S. (1983). *Trends Biochem. Sci.* **8**, 364-369.

IKEHARA, M., OHTSUKA, E., TOKUNAGA, T., NISHIKAWA, S., UESUGI, S., TANAKA, T., AOYAMA, Y., KIKYODANI, S., FUJIMOTO, K., YANASE, K., FUCHIMURA, K. & MORIOKA, H. (1986). *Proc. Natl Acad. Sci. USA*, **83**, 4695-4699.

JONES, T. A. (1978). *J. Appl. Cryst.* **11**, 268-272.

KATTI, S. K., SESHADRI, T. P. & VISWAMITRA, M. A. (1981). *Acta Cryst.* **B37**, 1825-1831.

KRATZIN, H. (1987). Personal communication.

LUZZATI, P. V. (1952). *Acta Cryst.* **5**, 802-810.

MACHIN, P. A., WONACOTT, A. J. & MOSS, D. (1983). *Daresbury News*, **10**, 3-9.

PONNUSWAMY, P. K. & MANAVALAN, P. (1976). *J. Theor. Biol.* **60**, 481-486.

QUAAS, R., CHOE, H.-W., HAHN, U., MCKEOWN, Y., STANSSENS, P., ZABEAU, M., FRANK, R. & BLÖCKER, H. (1987). *Biophosphates and their Analogues, Synthesis, Structure, Metabolism and Activity*, edited by K. S. BRUZIK & W. J. STEC, pp. 345-348. Amsterdam: Elsevier.

RAMACHANDRAN, G. N., RAMAKRISHNAN, C. & SASISEKHARAN, V. (1963). *J. Mol. Biol.* **7**, 95-99.

RAVICHANDRAN, V. & SUBRAMANIAN, E. (1981). *Int. J. Pept. Protein Res.* **18**, 121-126.

SUGIO, S., AMISAKI, T., OHISHI, H., TOMITA, K.-I., HEINEMANN, U. & SAENGER, W. (1985). *FEBS Lett.* **181**, 129-132.

SUGIO, S., OKA, K.-I., OHISHI, H., TOMITA, K.-I. & SAENGER, W. (1985). *FEBS Lett.* **183**, 115-118.

TAKAHASHI, K. (1971). *J. Biochem.* **70**, 945-960.

TAKAHASHI, K. (1985). *J. Biochem.* **98**, 815-817.

TAKAHASHI, K. & MOORE, S. (1982). In *The Enzymes*, Vol. 15, pp. 435-468. New York: Academic Press.

WILSON, A. J. C. (1942). *Nature (London)*, **150**, 151-152.

WLODAWER, A., BORKAKOTI, N., MOSS, D. S. & HOWLIN, B. (1986). *Acta Cryst.* **B42**, 379-387.